

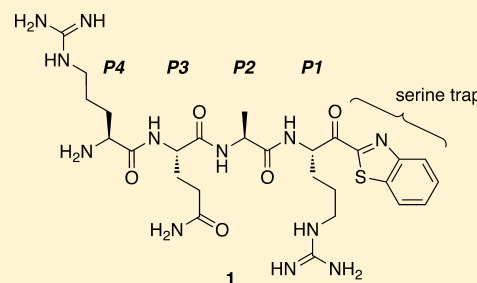
## Design and Synthesis of Potent, Selective Inhibitors of Matriptase

Éloïc Colombo,<sup>†</sup> Antoine Désilets,<sup>†</sup> Dominic Duchêne,<sup>‡</sup> Félix Chagnon,<sup>†</sup> Rafael Najmanovich,<sup>‡</sup> Richard Leduc,<sup>†</sup> and Eric Marsault<sup>\*,†</sup><sup>†</sup>Department of Pharmacology and <sup>‡</sup>Department of Biochemistry, Faculty of Medicine and Health Sciences, Université de Sherbrooke, 3001 12e Avenue Nord, Sherbrooke PQ, J1H5N4, Canada

## Supporting Information

**ABSTRACT:** Matriptase is a member of the type II transmembrane serine protease family. Several studies have reported deregulated matriptase expression in several types of epithelial cancers, suggesting that matriptase constitutes a potential target for cancer therapy. We report herein a new series of slow, tight-binding inhibitors of matriptase, which mimic the P1–P4 substrate recognition sequence of the enzyme. Preliminary structure–activity relationships indicate that this benzothiazole-containing RQAR-peptidomimetic is a very potent inhibitor and possesses a good selectivity for matriptase versus other serine proteases. A molecular model was generated to elucidate the key contacts between inhibitor **1** and matriptase.

**KEYWORDS:** matriptase, type II transmembrane serine protease, slow tight-binding inhibitor



Cell surface proteolysis is an important mechanism for the degradation or generation of biological effectors that engage various signaling pathways. Recently, a novel family of proteolytic enzymes called type II transmembrane serine proteases (TTSPs) has been associated with crucial roles in numerous physiological processes.<sup>1</sup> In humans, the 17 members of this family are divided into four subfamilies: HAT/DESC, Hepsin/TMPRSS, Corin, and matriptase.<sup>1</sup> These transmembrane proteases are structurally defined by a cytoplasmic amino-terminal region, a transmembrane domain, a stem region that contains various functional domains, and a carboxy-terminal extracellular serine protease domain of the chymotrypsin (S1) fold, characterized by the canonical histidine, aspartate, and serine catalytic triad essential for proteolytic activity. Matriptase, one of the most characterized TTSPs to date, is expressed in epithelial cells where it carries out essential functions in development, differentiation, and maintenance of epithelial barrier homeostasis. Matriptase knockout mice die shortly after birth due to severe dehydration caused by impaired epidermal barrier function, indicative of a crucial role in development.<sup>2</sup> Among the most recognized matriptase substrates are pro-hepatocyte growth factor,<sup>3</sup> pro-prostasin,<sup>4</sup> protease-activated receptor-2 (PAR-2),<sup>5</sup> pro-urokinase plasminogen activator,<sup>5</sup> CUB domain-containing protein-1,<sup>6</sup> and platelet-derived growth factor-D.<sup>7</sup>

Like many other proteases, the inactive zymogen precursor of matriptase needs to be converted to its active form. This is achieved via an initial cleavage occurring at residue Gly<sup>149</sup>, followed by an autoproteolytic cleavage at residue Arg<sup>614</sup> within the RQAR<sup>614</sup>-VVG sequence of the activation peptide of matriptase. Matriptase forms complexes with its cognate Kunitz type serine protease inhibitor, the hepatocyte growth factor activator inhibitor-1 (HAI-1), which is involved in activation, inhibition, expression, and trafficking of the enzyme.<sup>8</sup> Several

studies have shown that the proteolytic activity of matriptase must be tightly regulated during development, and deregulated matriptase activity has been linked to various pathologies. For example, a rare genetic skin disorder, autosomal recessive ichthyosis with hypotrichosis (ARIH), was found to be caused by mutations in the matriptase coding region, leading to the production of an inactive protease.<sup>9,10</sup> Elevated levels of matriptase in osteoarthritis are thought to facilitate the induction of cartilage destruction,<sup>11</sup> while lowered levels have been detected in colonic epithelia of inflammatory bowel disease patients.<sup>12</sup> Matriptase is overexpressed in a variety of epithelial cancers<sup>13</sup> and causes malignant transformations when orthotopically overexpressed in the skin of mice, suggesting a causal role in human carcinogenesis.<sup>14</sup> The latter findings suggest that deregulation of matriptase expression or activity is involved in the initiation and/or progression of cancer. Combined with its localization at the cellular surface of epithelial cells, matriptase appears as an attractive therapeutic target for the design and optimization of selective inhibitors to better understand its role in pathologies such as cancer. Several groups have been interested in the development of such inhibitors via different strategies.<sup>15–24</sup>

In this study, we report a new class of potent and selective peptidomimetic inhibitors of matriptase based on the P4–P1 (Arg-Gln-Ala-Arg) portion of the activation peptide of matriptase, to which was linked a carboxy-terminal serine trap in the form of a ketobenzothiazole group. The ketobenzothiazole serine trap was selected to form a covalent and reversible bond with the catalytic serine residue of the enzyme as reported

Received: February 28, 2012

Accepted: April 11, 2012

Published: April 11, 2012



by Costanzo et al. on thrombin.<sup>25</sup> The use of a serine trap is reminiscent of the recently approved HCV NS3-4A protease inhibitors Boceprevir and Telaprevir.<sup>26,27</sup> Herein, we report the synthesis, inhibitory activity, preliminary structure–activity relationships (SARs), and selectivity of this new class of inhibitors and propose a molecular model of inhibitor **1** docked into the active site of matriptase.

The inhibitor sequence is based on the natural autoactivation peptide sequence of matriptase Arg-Gln-Ala-Arg (RQAR) explored by our group,<sup>28</sup> to which was added a ketobenzothiazole serine trap (Figure 1).

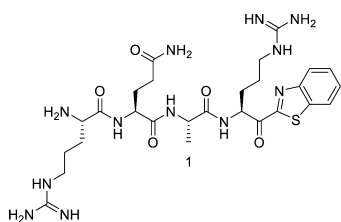
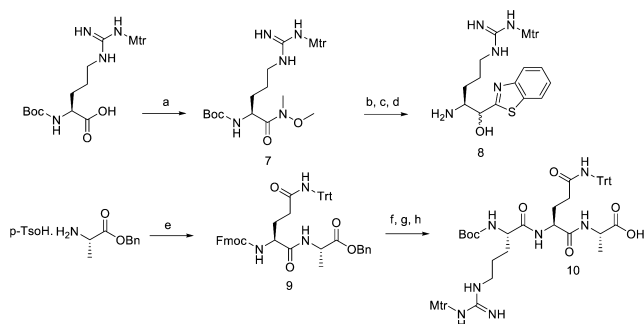


Figure 1. Chemical structure of inhibitor **1**.

Synthetically, inhibitor **1** and its analogues were assembled similarly to the method reported by Costanzo et al.<sup>25</sup> by peptide coupling of warhead-functionalized P1 fragment **8** with protected P4–P2 fragment **10** (Schemes 1 and 2). The

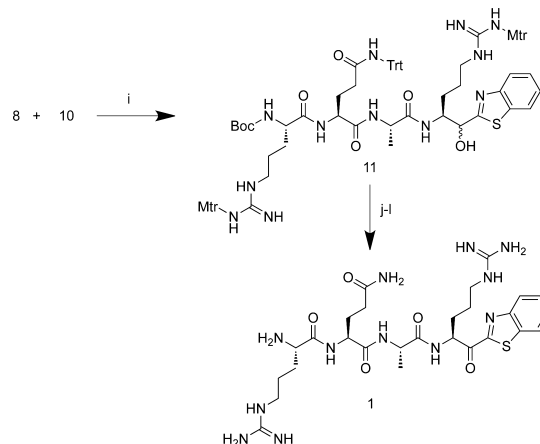
### Scheme 1. Synthesis of Tripeptide **11**<sup>a</sup>



<sup>a</sup>Reagents and conditions: (a) HN(Me)OMe, HATU, DIPEA, THF, r.t. (b) Benzothiazole, *n*-BuLi, THF, −78 °C. (c) NaBH<sub>4</sub> MeOH, −20 °C. (d) TFA/DCM 20:80, r.t. (e) Fmoc-Gln(Trt)-OH, HATU, DIPEA, THF, r.t. (f) Et<sub>3</sub>NH/DCM 20:80, r.t. (g) Boc-Arg(Mtr)-OH, EDC-HOBT, DCM, r.t. (h) H<sub>2</sub>, Pd/C (10%) EtOH, r.t.

synthesis of inhibitor **1** is shown as an example. First, fragment **8** carrying the serine trap was prepared from the corresponding Weinreb amide **7**, by addition of in situ generated 2-lithio-benzothiazole.<sup>25</sup> The resulting ketobenzothiazole was reduced in the same operation with NaBH<sub>4</sub> as a means of protecting the electrophilic keto group, and then, the Boc group was deprotected by acidolysis. On the other hand, *L*-Ala benzyl ester tosylate was coupled with Fmoc-Gln-OH using HATU to afford dipeptide **9**. After Fmoc removal, the crude dipeptide was coupled with Boc-Arg(Mtr)-OH in the presence of 1-ethyl-3-(3-dimethylaminopropyl) carbodiimide hydrochloride (EDC) and *N*-hydroxybenzotriazole (HOBT) to give the corresponding fully protected tripeptide. Benzyl ester hydrolysis then generated the desired fragment **10**. Subsequent coupling of tripeptide **10** with warhead **8** provided intermediate **11** (Scheme 2). The tetrapeptide scaffold **11** was then oxidized with 2-iodoxybenzoic acid (IBX),<sup>29</sup> followed by final acidolysis

### Scheme 2. Assembly of Fragments<sup>a</sup>



<sup>a</sup>Reagents and conditions: (i) HATU, DIPEA, DMF, r.t. (j) IBX, DMSO, r.t. (k) HF, anisole, 5 °C. (l) reverse phase prep HPLC.

of protective groups with HF. Compounds were generally obtained as a 8:2 mixtures of epimers,<sup>25</sup> which were separated by reverse-phase preparative high-performance liquid chromatography (HPLC). Structural analogues **2–7** (Table 1) were obtained according to the same synthetic method.

### Table 1. Preliminary SARs<sup>a</sup>

inhibitor	P <sub>4</sub> -P <sub>3</sub> -P <sub>2</sub> -P <sub>1</sub>		K <sub>i</sub> (nM)
	R <sub>1</sub> , R <sub>2</sub>		
<b>1</b>	R-Q-A-R	=O	0.011 <sup>tb</sup> ± 0.0004
<b>2</b>	R-Q-A-R	H, OH <sup>b</sup>	6124 <sup>mm</sup> ± 2702
<b>3</b>	R-Q-A-K	=O	9.5 <sup>tb</sup> ± 1.3
<b>4</b>	Q-A-R	=O	0.088 <sup>tb</sup> ± 0.010
<b>5</b>	A-R	=O	1.4 <sup>tb</sup> ± 0.3
<b>6</b>	R	=O	457 <sup>mm</sup> ± 132
<b>7</b>	R-Q-A-(D)R	=O	4.6 <sup>tb</sup> ± 0.8

<sup>a</sup>K<sub>i</sub> values were determined as described in the Materials and Methods (tb, tight binding; mm, mixed model). Measurements of enzymatic activity were performed in triplicate and represent the means ± standard deviations of at least three independent experiments. <sup>b</sup>A 3:2 mixture of diastereomers, absolute stereochemistry undetermined.

First, the inhibitory activity of tetrapeptide **1** toward matriptase was characterized. The progress curve for hydrolysis of a fluorogenic substrate by matriptase (1 nM) in the presence of compound **1** (2.5 nM) displays a biphasic curve with a rapid initial phase and a slower, steady-state phase (data not shown), suggesting reversible slow, tight-binding, or irreversible inhibition.

To further evaluate the inhibitor profile, the dissociation of the enzyme:inhibitor complex (EI) was investigated using dilution experiments.<sup>30</sup> Figure 2 reports the comparison of the dissociation curves for compound **1** (Figure 2A) and irreversible inhibitor Glu-Gly-Arg chloromethyl ketone (EGR-CMK) (Figure 2B). The dissociation curve of EGR-CMK displays a linear product versus time relationship, indicative of irreversible inhibition. Conversely, the dissociation curve of

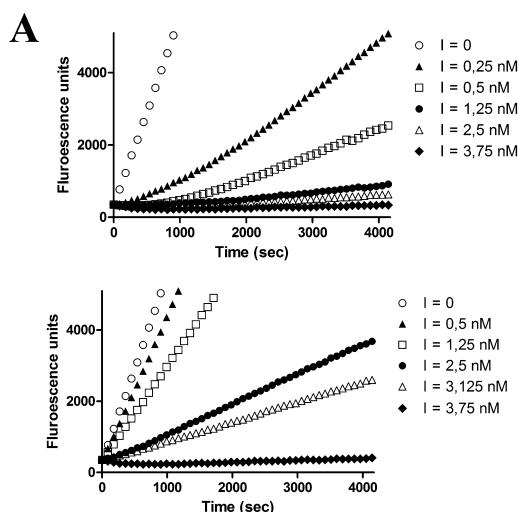


**Figure 2.** Dissociation of EI complex. Matriptase and increasing concentrations of (A) RQAR-Benzo or (B) EGR-CMK were preincubated for 20 min at room temperature and diluted 2000 times in reaction buffer containing 400  $\mu$ M Boc-QAR-AMC. The final concentration of matriptase is 0.25 nM and is varied as indicated for inhibitors. The proteolytic activity in the reaction buffer was measured as described in the Materials and Methods (see the Supporting Information).

inhibitor **1** shows an exponential shape, suggesting dissociation of the EI complex. Together, these data confirm the formation of a slow, tight-binding, and reversible complex between inhibitor and enzyme, as initially designed.

To further characterize matriptase inhibition by compound **1**, the inhibition constant ( $K_i$ ) was determined using the Morrison equation for reversible tight-binding inhibition.<sup>31</sup> In these conditions, the RQAR-ketobenzothiazole inhibitor **1** showed high potency for matriptase, with a  $K_i$  of 0.011 nM (Table 1). A preliminary analysis of SARs was subsequently performed by exploring the critical P1 position. To confirm the importance of the keto group for matriptase inhibition, we measured the inhibitory activity of a reduced form of the RQAR-ketobenzothiazole toward matriptase (compound **2**, Table 1). Reduced analogue **2** (3:2 mixture of diastereomers at the alcohol position, undetermined absolute stereochemistry) displayed very weak inhibition, as expected. Indeed, a stoichiometric ratio of I/E > 1000 was required to observe substantial inhibition, as testified by a  $K_i$  of 6.1  $\mu$ M, which contrasts with the much more potent oxidized form **1** and is consistent with a functional serine trap mechanism.

Table 1 reports the influence of structural variations of inhibitor **1** on matriptase inhibition. To ascertain the importance of stereochemistry at the P1 position, analogue R-Q-A-(D)R **7** was tested and displayed a 400-fold lower inhibition. Next, it is known that the TTSPs have a preference for basic residues (Lys or Arg) in position P1.<sup>28</sup> Accordingly, matriptase displays a preference for an Arg residue in position P1 by almost 3 orders of magnitude over Lys (3 vs 1,  $K_i$  0.011 vs 9.5 nM). Furthermore, to better ascertain the respective contribution of the P4, P3, and P2 residues on the inhibitory profile, the peptidic portion was truncated by one, two, and three residues starting from the N-terminal extremity (analogues **4–6**). Deletion of the P4 residue gave a compound that conserves the profile of a tight-binding inhibitor, yet with an 8-fold decreased potency as compared to **1** (**4**,  $K_i$  = 0.088 vs 0.011 nM). Inhibitor **5**, in which the P4 and P3 moieties were

simultaneously deleted, remains a tight-binding inhibitor with 127-fold reduced potency as compared to **1** ( $K_i$  = 1.4 vs 0.011 nM). Finally, inhibitor **6**, in which the P4–P2 tripeptide portion is removed, is dramatically less potent, with a  $K_i$  of 457 nM, over 30000-fold less potent than inhibitor **1**. Additionally, **6** no longer behaves as a tight-binding inhibitor but as an inhibitor possessing a mixed mode of inhibition as determined by global fitting analysis for different modes of inhibition (see the Supporting Information). Altogether, these results confirm the importance of residues at the P4–P2 positions for potent inhibition of matriptase.

The selectivity profile of inhibitor **1** for matriptase versus other serine proteases, including TTSPs, was subsequently determined (Table 2). Indeed, the selectivity of most published

**Table 2.** Selectivity Profile<sup>a</sup>

proteases	$K_i$ (nM)	selectivity ( $K_i$ other/ $K_i$ matriptase)
matriptase	0.011 <sup>tb</sup> $\pm$ 0.0004	
matriptase-2	3.3 <sup>tb</sup> $\pm$ 1.0	300
hepsin	1.1 <sup>tb</sup> $\pm$ 0.3	100
TMPRSS11D	8.4 <sup>tb</sup> $\pm$ 2.6	764
trypsin	0.97 <sup>tb</sup> $\pm$ 0.17	88
thrombin	637 <sup>mm</sup> $\pm$ 131	>30,000
furin	NI (10 $\mu$ M)	

<sup>a</sup> $K_i$  values were determined as described in the Materials and Methods (tb, tight binding; mm, mixed model; and NI, no inhibition). Enzymatic measurements were performed in triplicate and represent the mean  $\pm$  standard deviation of at least three independent experiments.

matriptase inhibitors has not been reported versus other TTSPs. Experimental  $K_i$  values were determined as described in the Materials and Methods (see the Supporting Information) for inhibitor **1** against other TTSPs (hepsin, matriptase-2, and TMPRSS11D) and serine proteases (trypsin and thrombin). Selectivity was expressed as the ratio of  $K_i$  values. Compound **1** was found to be highly selective for matriptase versus other enzymes: trypsin (88-fold), hepsin (100-fold), matriptase-2 (300-fold), TMPRSS11D (764-fold), thrombin (>30000-fold), and furin (no inhibition). This high level of selectivity of the RQAR-benzothiazole sequence for matriptase relative to other trypsin-like proteases is remarkable. Although at this stage the structural reasons for such selectivity are not elucidated, additional studies, including molecular modeling and crystallography, are underway to provide an explanation for this level of selectivity.

To understand the preferred mode of docking of inhibitor **1** in the active site of matriptase and rationalize SARs, a molecular model of inhibitor **1** docked in the published X-ray structure of matriptase was built (Figure 3). According to this docking model, the side chain of residue Arg in P1 is highly stabilized in a network of hydrogen bonds, which includes a salt bridge with matriptase residue Asp<sup>799</sup>, a hydrogen bond with Ser<sup>800</sup>, and hydrogen bonds with the backbone amide of Gly<sup>827</sup> and Gly<sup>829</sup>. This may account for the preference of Arg over Lys in P1, particularly since the S1 pocket seems to be best suited to accommodate the side chain of Arg instead of Lys, which is longer and possesses reduced hydrogen bond capability as compared to Arg. Residue Ala in P2 of inhibitor **1** lays over Phe<sup>708</sup>, which separates the S2 and the S4 pockets. This pocket is quite nonpolar due to the presence of the Phe<sup>708</sup> residue. It can also accommodate larger residues, in agreement with our

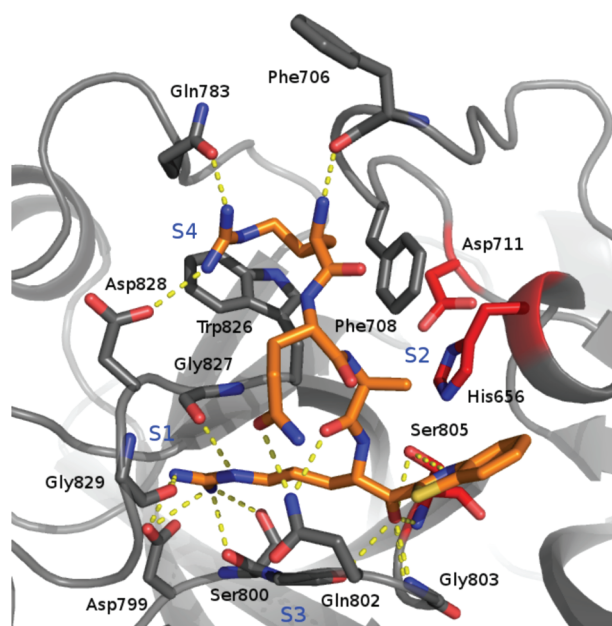


**Figure 3.** Docking of inhibitor **1** in the active site of matriptase. Matriptase<sup>32</sup> is shown in gray and residues within the active site. Inhibitor **1** is shown in orange. Catalytic triad residues are shown in red. The image was generated using Pymol.<sup>33</sup> Numbers refer to matriptase numbering.

previous results on substrate preference, which demonstrated that the S2 pocket could accommodate residues as large as Arg or Tyr.<sup>28</sup> The side chain of residue Gln in P3 of inhibitor **1** bridges over the Arg residue in P1 to interact with Gln<sup>802</sup> in the S3 pocket. Next, the side chain of the Arg residue in P4 of inhibitor **1** interacts with the side chain of Asp<sup>828</sup> of matriptase via a salt bridge. It also interacts via hydrogen bonding with Gln<sup>783</sup>. Finally, the catalytic Ser<sup>805</sup> residue is adequately positioned in the vicinity of the carbonyl moiety of the ketobenzothiazole group to form a covalent, reversible bond in the form of a hemiacetal. The oxygen atom of the carbonyl group is stabilized via hydrogen bonding with the backbone amides of residues Gly<sup>803</sup> and Ser<sup>805</sup>.

In conclusion, we herein report a new series of potent, peptidomimetic inhibitors of matriptase. We have demonstrated that a tetrapeptide scaffold based on the natural autoactivation sequence of matriptase is suitable for the design of potent slow, tight-binding inhibitors with sub-nanomolar potency. Moreover, inhibitor **1** possesses a high level of selectivity for matriptase versus other serine proteases, including TTSPs. Efforts are underway to further improve the profile of this inhibitor, to account for the observed level of selectivity and use it to validate the role of matriptase in several diseases..

## ■ ASSOCIATED CONTENT

### 📄 Supporting Information

Synthetic procedures, characterization data, biological methods, and molecular modeling procedures. This material is available free of charge via the Internet at <http://pubs.acs.org>.

## ■ AUTHOR INFORMATION

### Corresponding Author

\*E-mail: [Eric.Marsault@Usherbrooke.ca](mailto:Eric.Marsault@Usherbrooke.ca).

## Funding

We thank Université de Sherbrooke and the Canadian Institutes of Health Research for financial support (CIHR, MOP-97964). CREPSUS (Centre de Recherche en Pharmacologie Structurale de l'Université de Sherbrooke) is gratefully acknowledged for a scholarship to D.D.

## Notes

The authors declare no competing financial interest.

## ■ ACKNOWLEDGMENTS

Professors B. Guerin and Y. Dory are acknowledged for sharing purification equipment.

## ■ ABBREVIATIONS

DIPEA, *N,N*-diisopropylethylamine; EDC, 1-ethyl-3-(3-dimethylaminopropyl) carbodiimide hydrochloride; HOBT, *N*-hydroxybenzotriazole; IBX, 2-Iodoxybenzoic acid; THF, tetrahydrofuran; DCM, dichloromethane; EtOH, ethanol; TFA, trifluoroacetic acid; MeOH, methanol; DMF, dimethylformamide; DMSO, dimethylsulfoxide; *n*-Buli, *n*-butyllithium; HPLC, high-performance liquid chromatography

## ■ REFERENCES

- (1) Antalis, T. M.; Bugge, T. H.; Wu, Q. Membrane-anchored serine proteases in health and disease. *Prog. Mol. Transl. Sci.* **2011**, *99*, 1–50.
- (2) List, K.; Haudenschild, C. C.; Szabo, R.; Chen, W.; Wahl, S. M.; Swaim, W.; Engelholm, L. H.; Behrendt, N.; Bugge, T. H. Matriptase/MT-SP1 is required for postnatal survival, epidermal barrier function, hair follicle development, and thymic homeostasis. *Oncogene* **2002**, *21*, 3765–3779.
- (3) Lee, S. L.; Dickson, R. B.; Lin, C. Y. Activation of hepatocyte growth factor and urokinase/plasminogen activator by matriptase, an epithelial membrane serine protease. *J. Biol. Chem.* **2000**, *275*, 36720–36725.
- (4) Netzel-Arnett, S.; Currie, B. M.; Szabo, R.; Lin, C. Y.; Chen, L. M.; Chai, K. X.; Antalis, T. M.; Bugge, T. H.; List, K. Evidence for a matriptase-proteasome proteolytic cascade regulating terminal epidermal differentiation. *J. Biol. Chem.* **2006**, *281*, 32941–32945.
- (5) Takeuchi, T.; Harris, J. L.; Huang, W.; Yan, K. W.; Coughlin, S. R.; Craik, C. S. Cellular localization of membrane-type serine protease1 and identification of protease-activated receptor-2 and single-chain urokinase-type plasminogen activator as substrates. *J. Biol. Chem.* **2000**, *275*, 26333–26334.
- (6) He, Y.; Wortmann, A.; Burke, L. J.; Reid, J. C.; Adams, M. N.; Abdul-Jabbar, I.; Quigley, J. P.; Leduc, R.; Kirchhofer, D.; Hooper, J. D. Proteolysis-induced N-terminal ectodomain shedding of the integral membrane glycoprotein CUB domain-containing protein 1 (CDCP1) is accompanied by tyrosine phosphorylation of its C-terminal domain and recruitment of Src and PKCdelta. *J. Biol. Chem.* **2010**, *285*, 26162–26173.
- (7) Ustach, C. V.; Huang, W.; Conley-LaComb, M. K.; Lin, C. Y.; Che, M.; Abrams, J.; Kim, H. R. A novel signalling axis of matriptase/PDGF-D/B-PDGFR in human prostate cancer. *Cancer Res.* **2010**, *70*, 9631–9640.
- (8) Oberst, M. D.; Chen, L. Y.; Kiyomiya, K.; Williams, C. A.; Lee, M. S.; Johnson, M. D.; Dickson, R. B.; Lin, C. Y. HAI-1 regulates activation and expression of matriptase, a membrane-bound serine protease. *Am. J. Physiol. Cell. Physiol.* **2005**, *289*, 462–470.
- (9) Basel-Vanagaite, L.; Attia, R.; Ishida-Yamamoto, A.; Rainshtein, L.; Ben Amitai, D.; Lurie, R.; Pasmanik-Chor, M.; Indelman, M.; Zvulunov, A.; Saban, S.; Magal, N.; Sprecher, E.; Shohat, M. Autosomal recessive ichthyosis with hypotrichosis caused by mutation in ST14, encoding type II transmembrane serine protease matriptase. *Am. J. Hum. Genet.* **2007**, *80*, 467–477.
- (10) Désilets, A.; Béliveau, F.; Vandal, G.; McDufflo, F. O.; Lavigne, P.; Leduc, R. Mutation G827R in matriptase causing autosomal

recessive ichthyosis with hypotrichosis yields an inactive protease. *J. Biol. Chem.* **2008**, *283*, 10535–10542.

(11) Milner, J. M.; Patel, A.; Davidson, R. K.; Swingler, T. E.; Désilets, A.; Young, D. A.; Kelso, E. B.; Donell, S. T.; Cawston, T. E.; Clark, I. M.; Ferrell, W. R.; Plevin, R.; Lockhart, J. C.; Leduc, R.; Rowan, A. D. Matriptase is a novel initiator of cartilage matrix degradation in osteoarthritis. *Arthritis Rheum.* **2010**, *61*, 1955–1966.

(12) Netzel-Arnett, S.; Buzza, M. S.; Shea-Donohue, T.; Désilets, A.; Leduc, R.; Fasano, A.; Bugge, T. H.; Antalis, T. M. Matriptase protects against experimental colitis and promotes intestinal barrier recovery. *Inflamm. Bowel Dis.* **2011**, DOI: 10.1002/ibd.21930.

(13) List, K. Matriptase: A culprit in cancer? *Future Oncol.* **2009**, *5*, 97–104.

(14) List, K.; Szabo, R.; Molinolo, A.; Sriuranpong, V.; Redeye, V.; Murdock, T.; Burke, B.; Nielsen, B. S.; Gutkind, J. S.; Bugge, T. H. Deregulated matriptase causes ras-independent multistage carcinogenesis and promotes ras-mediated malignant transformation. *Genes Dev.* **2005**, *19*, 1934–1950.

(15) Galkin, A. V.; Mullen, L.; Fox, W. D.; Brown, J.; Duncan, D.; Moreno, O.; Madison, E. L.; Agus, D. B. CVS-3983, a selective matriptase inhibitor, suppresses the growth of androgen independent prostate tumor xenografts. *Prostate* **2004**, *3*, 228–235.

(16) Stoop, A. A.; Craik, C. S. Engineering of macromolecular scaffold to develop specific protease inhibitors. *Nat. Biotechnol.* **2003**, *21*, 1063–1068.

(17) Désilets, A.; Longpré, J. M.; Beaulieu, M. E.; Leduc, R. Inhibition of Human matriptase by eglin c variants. *FEBS Lett.* **2006**, *580*, 2227–2232.

(18) Li, P.; Jiang, S.; Lee, S. L.; Lin, C. Y.; Johnson, M. D.; Dickson, R. B.; Michejda, C. J.; Roller, P. Design and Synthesis of novel and potent inhibitors of the type II transmembrane protease, matriptase, based upon the sunflower Trypsin inhibitor-1. *J. Med. Chem.* **2007**, *50*, 5976–5983.

(19) Long, Y. Q.; Lee, S. L.; Lin, C. Y.; Enyedy, I. J.; Wang, S.; Li, P.; Dickson, R. B.; Peter, P. R. Synthesis and Evaluation of the sunflower derived trypsin inhibitor as a potent inhibitor of the type II transmembrane serine protease, matriptase. *Bioorg. Med. Chem. Lett.* **2001**, *11*, 2515–2519.

(20) J. Enyedy, I.; Sheau-Ling, L.; Kuo, A. H.; Dickson, R. B.; Lin, C. Y.; Wang, S. Structure based approach for discovery of bis-benzamidines as novel inhibitors of matriptase. *J. Med. Chem.* **2001**, *44*, 1349–1355.

(21) Jiang, S.; Li, P.; Lee, S. L.; Lin, C. Y.; Long, Y. Q.; Johnson, M. D.; Dickson, R. B.; Roller, P. P. Design and synthesis of redox stable analogues of sunflower trypsin inhibitors (SFTI-1) on solid support, potent inhibitors of matriptase. *Org. Lett.* **2007**, *9*, 9–12.

(22) Steinmetzer, T.; Dönnecke, D.; Korsonewski, C.; Steinmetzer, P.; Schuzle, A.; Martin Saupe, S.; Scheweinitz, A. Modification of the N-terminal sulfonyl residue in 3-amidinophenylalanine-based on matriptase inhibitors. *Bioorg. Med. Chem. Lett.* **2009**, *19*, 67–73.

(23) Steinmetzer, T.; Schuzle, A.; Stürzebecher, A.; Dönnecke, D.; Uhland, K.; Schuster, O.; Steinmetzer, P.; Müller, F.; Friedrich, R.; Than, M. E.; Bode, W.; Stürzebecher, J. Secondary Amides of sulfonated 3-amidinophenylalanine. New potent and selective inhibitors of matriptase. *J. Med. Chem.* **2006**, *49*, 4116–4126.

(24) Tekeste Sisay, M.; Steinmetzer, T.; Stimberg, M.; Hammami, M.; Bajorath, J.; Gütschow, M. Identification of the first low-molecular-weight of matriptase-2. *J. Med. Chem.* **2010**, *53*, 5523–5535.

(25) Costanzo, M. J.; Almond, H. R., Jr.; Hecker, L. R.; Schott, M. R.; Yabut, S. C.; Zhang, H. C.; Andrade-Gordon, P.; Corcoran, T. W.; Giardino, E. C.; Kauffman, J. A.; Lewis, J. M.; de Garavilla, L.; Haertlein, B. J.; Maryanoff, B. E. In-depth study of tripeptide based alpha-ketoheterocycles as inhibitors of thrombin. Effective utilization of the S1' subsite and its implications to structure-based drug design. *J. Med. Chem.* **2005**, *48*, 1984–2008.

(26) Venkatraman, S.; Bogen, S. L.; Arasappan, A.; Bennett, F.; Chen, K.; Jao, E.; Liu, Y. T.; Lovey, R.; Hendrata, S.; Huang, Y.; Pan, W.; Parekh, T.; Pinto, P.; Popov, V.; Pike, R.; Ruan, S.; Santhanam, B.; Vibulban, B.; Wu, W.; Yang, W.; Kong, J.; Liang, X.; Wong, J.; Liu, R.;

Butkiewicz, N.; Chase, R.; Hart, A.; Agrawal, S.; Ingravallo, P.; Pichardo, J.; Kong, R.; Baroudy, B.; Malcom, B.; Guo, Z.; Prongay, A.; Madison, V.; Broske, L.; Cui, X.; Cheng, K. C.; Hsieh, Y.; Brisson, J. M.; Prelusky, D.; Korfmacher, W.; White, R.; Bogdanowich-Knipp, S.; Pavlosky, A.; Bradley, P.; Saksena, A. K.; Ganguly, A.; Piwinski, J.; Girijavallabhan, V.; Njoroge, F. G. Discovery of (1R,5S)-N-[3-amino-1-(cyclobutylmethyl)-2,3-dioxopropyl]-3-[[[(1,1-dimethylethyl)-amino]carbonyl]amino]-3,3-dimethyl-1-oxobutyl]-6,6-dimethyl-3-azabicyclo[3.1.0]hexan-2(S)-carboxamide (SCH503034), a selective, potent, orally bioavailable hepatitis C virus NS3 protease inhibitor: a potential therapeutic agent for the treatment of hepatitis C infection. *J. Med. Chem.* **2006**, *49*, 6074–6086.

(27) Kwong, A. D.; Kauffman, R. S.; Hurter, P.; Mueller, P. Discovery and development of telaprevir: an NS3-4A protease inhibitor for treating genotype 1 chronic hepatitis C virus. *Nat. Biotechnol.* **2001**, *29*, 993–1003.

(28) Béliveau, F.; Désilets, A.; Leduc, R. Probing the substrate specificities of matriptase, matriptase-2, hepsin and DESC1 with internally quenched fluorescent peptides. *FEBS J.* **2009**, *276*, 2213–2226.

(29) Frigerio, M.; Santagostimo, M.; Sputore, S.; Palmisano, G. Oxidation of Alcohols with o-Iodoxybenzoic Acid (IBX) in DMSO: A New Insight into an Old Hypervalent Iodine Reagent. *J. Org. Chem.* **1995**, *60*, 7272–7276.

(30) Copeland, R. *A Practical Introduction to Structure, Mechanism and Data Analysis*; Wiley-VCH: New-York, 2000; Chapter 10, pp 1–397.

(31) Bieth, J. G. Theoretical and practical aspects of proteinase inhibition kinetics. *Methods Enzymol.* **1995**, *248*, 59–84.

(32) Berman, H. M.; Westbrook, J.; Feng, Z.; Gilliland, G.; Bhat, T. N.; Weissig, H.; Shindyalov, I. N.; Bourne, P. E. The Protein Data Bank. *Nucleic Acids Res.* **2000**, *28*, 235–242.

(33) The PyMOL Molecular Graphics System, Version 1.2r1pre; Schrödinger, LLC, 26.